THERMAL AND EXERGETIC INVESTIGATION OF A SOLAR DISH COLLECTOR OPERATING WITH MONO AND HYBRID NANOFLUIDS

by

Saša R. PAVLOVIĆ[a*], Evangelos BELLOS[b], Velimir P. STEFANOVIĆ[a], Milan M. DJORDJEVIĆ[c], and Darko M. VASILJEVIĆ[d]

[a] Department of Energetics and Process Technique, Faculty of Mechanical Engineering, University in Nis, Nis, Serbia
[b] Thermal Department, School of Mechanical Engineering, National Technical University of Athens, Greece
[c] Faculty of Technical Sciences, University of Pristina, Kosovska Mitrovica, Serbia
[d] Photonic Center, Institute of Physics, University of Belgrade, Belgrade, Serbia

Original scientific paper
https://doi.org/10.2298/TSCI18S5383P

The use of solar dish thermal collectors is a promising choice for designing sustainable energy systems. The use of nanofluids is a new way for enhancing the thermal performance of solar collectors because of their improved thermal properties. The objective of this study is to investigate the use of mono and hybrid nanofluids in a solar dish collector in order to determine which kind of nanofluids leads to higher performance enhancements. The analysis is conducted with a developed thermal model in Engineering Equation Solver and the collector is studied thermally and exergetically. The examined hybrid nanofluid has as base fluid syltherm 800 with 1% Cu and 1% TiO_2. Moreover, the examined mono nanofluids are the syltherm 800 with 2% Cu and syltherm 800 with 2% TiO_2. The investigated solar dish collector has a spiral absorber and it is examined for inlet temperatures from 25 °C up to 300 °C with a flow rate of 200 L/h. According to the final results, the use of hybrid nanofluid leads to higher thermal efficiency enhancement compared to the mono nanofluids because of the higher increase in the Nusselt number in the flow. More specifically, the use of the hybrid nanofluids leads to 0.99% mean thermal efficiency enhancement compared to the pure oil case, while the use of Oil/Cu and Oil/TiO_2 lead to 0.42% and to 0.56% mean thermal efficiency enhancement, respectively. Moreover, the exergy efficiency is found enhanced with the use of all nanofluids. The mean exergy efficiency enhancement is 1.21% with the hybrid nanofluid, while it is 0.73% with Oil/TiO_2 and 0.53% with Oil/Cu.

Key words: *solar dish collector, nanofluids, thermal analysis, exergy, hybrid nanofluid*

Introduction

Solar energy utilization is vital for achieving the sustainability and facing important dangers as the fossil fuel depletion [1], the global warming [2] and the increasing worldwide energy demand [3]. Solar thermal dish collector is a concentrating kind of solar collector which is able to produce useful heat at medium and high-temperature levels [4, 5]. Solar dish

* Corresponding author, e-mail: saledoca@gmail.com

collector has been used in a great range of applications as heating, cooling, drying, desalination electricity production, industrial heat and chemical processes [6, 7].

In the literature, there are numerous studies which investigate solar dish thermal collector performance. Moreover, there are many different examined configurations of solar dish collectors. Loni *et al.* [8] studied a rectangular-cavity tubular receiver in a solar dish collector in order to feed an Organic Rankine Cycle with the demanded heat input. They optimized the shape of the cavity and they proved that there is optimum cavity diameter which leads high optical efficiency and low thermal losses. Reddy *et al.* [9] studied a modified cavity receiver of a solar dish collector with a developed numerical model for the determining natural convection heat losses of the receiver. This configuration includes a tube wound in a hemispherical geometry which is covered with insulation to reduce the thermal losses. Przenzak *et al.* [10] examined a solar dish collector with two optical elements and a curved radiation absorber. They designed this collector for operation in high-temperature levels and there was a special design for achieving this goal. Zhu *et al.* [11] designed a pressurized volumetric solar receiver with a dish reflector for different mass-flow rates. They found the maximum exergetic efficiency of their system to be 36%. Daabo *et al.* [12] compared three receiver geometries: cylindrical, conical, and spherical. In every case, a helical tube was used in order to utilize the solar energy. Finally, they found that the conical shape is the best choice among the examined cases. Lastly, Yu *et al.* [13] studied a configuration with 31 small dishes as the concentrators of a volumetric tubular receiver.

The use of nanofluids is an interesting idea for enhancing the performance of solar dish collectors. The nanofluid-based solar dish collectors are examined in the last years and there are some literature studies in this field. Loni *et al.* [14] examined a cylindrical cavity receiver which operates with four oil-based nanofluids for nanoparticle concentrations up to 5%. According to their results, the use of Oil/Cu nanofluid is the most appropriate case with 38% exergy efficiency enhancement. Moreover, Loni *et al.* [15] found the water/CuO nanofluid to be the best case in a solar dish collector with the spiral receiver. Pavlovic *et al.* [16] found that the nanofluids with Cu as nanoparticle to be the best case. Pakhare *et al.* [17] studied experimentally the water/Al_2O_3 nanofluid and they found 10% thermal efficiency enhancement. Rajendran *et al.* [18] examined experimentally the water/SiC nanofluid in a solar dish collector and according to their results, there is high-performance enhancement close to 76%.

An alternative choice is the use of hybrid nanofluids which consist of more than one nanoparticle. This alternative nanofluid is able to lead to higher performance for two reasons. The first one is the achievement of superior thermal properties because different nanoparticles can be optimally combined. The second reason is that the hybrid nanofluids present different hydrodynamic and heat transfer properties, compared to the mono nanofluids due to synergetic effects [19]. Thus, the investigation of hybrid nanofluids is something important and promising. In the literature, there are only a few studies with hybrid nanofluids in concentrating collectors. Only [20, 21] exist which are associated with the use of hybrid nanofluids in parabolic trough solar collectors. These studies proved that the use of hybrid nanofluids leads to performance enhancement and especially [20] proved that the hybrid nanofluids leads to higher performance than the mono (or single) nanofluids with one nanoparticle kind.

In this direction, this study investigates the use of mono and hybrid nanofluids in a solar dish collector. To our knowledge, there is no other study which investigates the use of hybrid nanofluids in solar dish collectors. Moreover, the previous analysis proves that the investigation of this nanofluid kind is interesting and it is needed in the literature. The examined solar dish collector has a spiral absorber inside the housing and this system has been examined for operation with conventional fluids (experimentally and numerically) in the [22-26]. The examined nanofluids have Syltherm 800 (thermal oil) as the base fluid in order for the system to be examined in medium-high temperature levels. The use of Oil/TiO_2, Oil/Cu, and Oil/(TiO_2-Cu) nanofluids is performed, as well as the operation with pure thermal oil is examined. The system is studied for inlet temperatures from 25 °C up to 300 °C. The analysis is conducted with a developed thermal model in Engineering Equation Solver (EES) [27] which is validated with experimental results.

Material and methods

The examined solar collector

The examined collector is depicted in fig. 1. Figure 1(a) gives the total collector (receiver and concentrator), while fig. 1(b) shows the spiral cavity receiver. The real experimental set-up is located in the solar laboratory of the Faculty of Mechanical Engineering at the University of Nis (latitude 43°19' and longitude 21°54'). The solar dish has 11 petals while the 12th is missing in order to have the bracket. The receiver is a spiral tube which is located inside a metallic housing. Totally there are 13 coils in the receiver and the tube is corrugated. More detailed about this system can be found in [22-26]. It is important to state that there is a two-axis tracking system in order for the solar dish collector to follow the Sun during its operation. The base fluid in this collector is Syltherm 800 [28] which can operate up to 400 °C with a safety. The examined solar collector has an optical efficiency of 69% [22]. More specifically, the absorbance is 80% [23], the intercept factor 96% [26], and the reflectance 90%. This reflectance can be achieved with the Vega WR193 reflecting material [29]. The concentration ratio is 28.26 and the total aperture is 10.29 m^2.

The solar collector is investigated for inlet temperatures from 25 °C up to 300 °C with a flow rate of 200 L/h [23, 24]. The analysis is conducted with a developed model in EES [27] and the model has been validated in previous works [22-24].

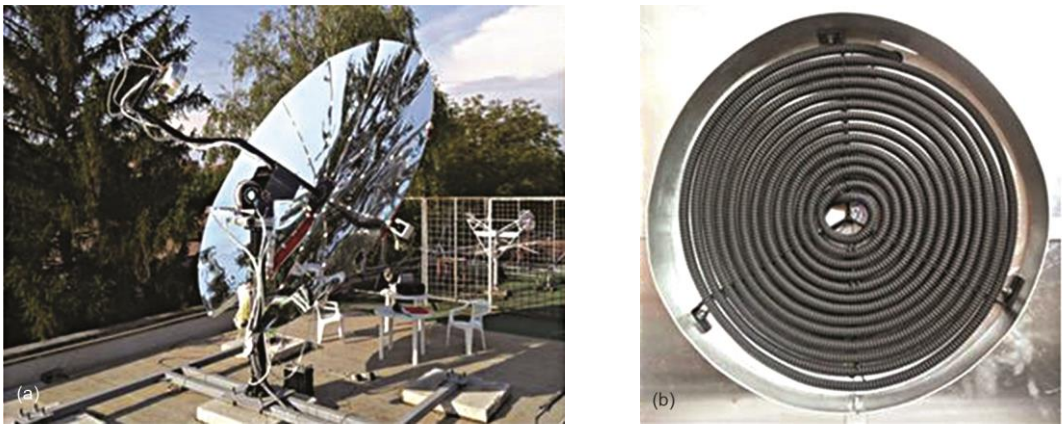

Figure 1. The experimental set-up of the solar dish collector; (a) the total collector, (b) the examined absorber

Thermal modeling

The thermal modeling of the present collector has been presented also in [22-24] and thus only the most important are given in this section. The thermal efficiency, η_{th}, is the ratio of the useful heat production, Q_u, to the solar energy, Q_s. The useful heat production can be calculated using the energy balance in the fluid volume while the solar energy using only the direct beam solar irradiation.

$$\eta_{th} = \frac{Q_u}{Q_s} = \frac{m\ c_p\ (T_{out} - T_{in})}{A_a\ G_b} \tag{1}$$

The exergy efficiency of the solar collector is calculated using the Petela model for the direct beam solar irradiation [30]:

$$\eta_{ex} = \frac{Q_u - m\ c_p\ T_o \ln\left(\frac{T_{out}}{T_{in}}\right)}{Q_s\left[1 - \frac{4}{3}\frac{T_o}{T_{Sun}} + \frac{1}{3}\left(\frac{T_o}{T_{Sun}}\right)^4\right]} \tag{2}$$

The reference temperature, T_o, is 298.15 K and the Sun temperature, T_{Sun}, 5770 K. It is important to state that the temperature levels in eq. (2) are all in Kelvin units.

The energy balance in the solar collector can be written as eq. (3). The optical efficiency, η_{opt}, is 69% [22].

$$Q_s\ \eta_{opt} = Q_u + Q_{loss} \tag{3}$$

The thermal losses, Q_{loss}, are radiation and convection thermal losses:

$$Q_{loss} = A_r\ h_{out}(T_r - T_{am}) + A_r\ \varepsilon_r\ \sigma(T_r^4 - T_{am}^4) \tag{4}$$

The h_{out} can be selected at 10 W/m^{2}K, the ε_r at 0.15 while σ is the Stefan-Boltzmann constant (σ = 5.67·10^{-8} W/m^{4}K). Moreover, it is important to state that the ambient temperature, T_{am}, is 25 °C, or 298 K for eq. (4), while the solar direct beam irradiation, G_b = 1000 W/m^2.

The heat transfer between the receiver and the fluid can be written as eq. (5). The mean fluid temperature is assumed to be the mean value of the inlet and outlet temperatures.

$$Q_u = A_r\ h(T_r - T_{fm}) \tag{5}$$

Nanofluid modeling

The mathematical modeling for the nanofluid thermal properties is presented. The density of the nanofluid is calculated as eq. (6). The base fluid is symbolized with "bf", the nanofluid with "nf", and the nanoparticle with "np". It is important to state that the volumetric nanoparticle concentration is symbolized with φ [31, 32]:

$$\rho_{nf} = \varphi\rho_{np} + (1-\varphi)\rho_{bf} \tag{6}$$

The specific heat capacity is calculated [32, 33]:

$$c_{p,nf} = \frac{\varphi\ \rho_{np}c_{p,np} + (1-\varphi)\rho_{bf}\,c_{pbf}}{\rho_{nf}} \tag{7}$$

The thermal conductivity is calculated with the Maxwell formula for spherical nanoparticles [34]:

$$k_{\mathrm{nf}} = k_{\mathrm{bf}} \frac{k_{\mathrm{np}} + 2k_{\mathrm{bf}} + 2\varphi(k_{\mathrm{np}} - k_{\mathrm{bf}})}{k_{\mathrm{np}} + 2k_{\mathrm{bf}} - \varphi(k_{\mathrm{np}} - k_{\mathrm{bf}})} \tag{8}$$

The nanofluid viscosity is calculated using the Bachelor model [35]:

$$\mu_{\mathrm{nf}} = \mu_{\mathrm{bf}}(1 + 2.5\varphi + 6.2\varphi^2) \tag{9}$$

For the hybrid nanofluid, eqs. (6)-(9) can be also used but the equivalent nanoparticle thermal properties have to be used. It can be assumed that there are two nanoparticles which are symbolized with "np1" and "np2", while the equivalent nanoparticle is symbolized with "np". The same strategy has been followed in [20]. Firstly, it can be said that the total concentration is calculated:

$$\varphi = \varphi_1 + \varphi_2 \tag{10}$$

The equivalent nanoparticle density is given:

$$\rho_{\mathrm{nf}} = \frac{\varphi_1 \rho_{\mathrm{np1}} + \varphi_2 \rho_{\mathrm{np2}}}{\varphi} \tag{11}$$

The equivalent nanoparticle specific heat capacity is given:

$$c_{p,\mathrm{np}} = \frac{\varphi_1 \rho_{\mathrm{np1}} c_{p,\mathrm{np1}} + \varphi_2 \rho_{\mathrm{np2}} c_{p,\mathrm{np2}}}{\varphi \rho_{\mathrm{np}}} \tag{12}$$

The equivalent nanoparticle thermal conductivity is given:

$$k_{\mathrm{nf}} = \frac{\varphi_1 k_{\mathrm{np1}} + \varphi_2 k_{\mathrm{np2}}}{\varphi} \tag{13}$$

In the present paper, the total concentration is kept at 2%. This assumption means that for the Oil/TiO_2 the φ is 2%, for the Oil/Cu the φ is 2%, while for the Oil/(TiO_2-Cu) the total φ is 2% with $\varphi_1 = 1\%$ and $\varphi_2 = 1\%$. Furthermore, it is important to state that the flow is turbulent in all the cases (Re > 2300). The heat transfer coefficient in the flow, *h*, is calculated using the Nusselt number for turbulent flow according to the next equation:

$$\mathrm{Nu} = \frac{hD}{k} \tag{14}$$

The characteristic flow parameter is the tube diameter, *D*, which is 10.5 mm.

The Nusselt number for the pure oil case is calculated according to the Dittus-Boelter equation [36] for turbulent flow:

$$\mathrm{Nu} = 0.023\,\mathrm{Re}^{0.8}\,\mathrm{Pr}^{0.4} \tag{15}$$

The Nusselt number for the nanofluid with Cu is calculated according to the Li and Xuan [37] formula for concentration up to 2% and turbulent flow:

$$\mathrm{Nu} = 0.4328[1 + 11.285\varphi^{0.754}(\mathrm{Re}_d\,\mathrm{Pr})^{0.218}]\,\mathrm{Re}^{0.333}\,\mathrm{Pr}^{0.4} \tag{16}$$

The nanoparticle diameter, d_p, is selected at 50 nm while the k_b is the Boltzmann's constant (~$1.3806\cdot10^{-23}$ J/K). The value of Reynolds number is a typical one because the nanoparticle diameters are usually between 5 nm and 100 nm.

$$\mathrm{Re}_d = \frac{2\rho_{\mathrm{bf}}\, k_b (T+273)}{\pi \mu_{\mathrm{bf}}^2\, d_p} \tag{17}$$

The Nusselt number for the nanofluid with TiO_2 is calculated according to the model of Duangthongsuk and Wongwises [38] for concentration up to 2% and turbulent flow:

$$\mathrm{Nu} = 0.074\,\mathrm{Re}^{0.707}\,\mathrm{Pr}^{0.385}(100\,\varphi)^{0.074} \tag{18}$$

The Nusselt number for the hybrid nanofluid with Cu-TiO_2 for concentration up to 2% and turbulent flow is calculated according to the Madhesh *et al.* model [39]:

$$\mathrm{Nu} = 0.012\,\mathrm{Re}\,\mathrm{Pr}^{0.33}(100\,\varphi)^{0.032} \tag{19}$$

The basic information of the examined nanoparticles is included in tab. 1.

Table 1. Basic information on the examined nanoparticles [40]

Nanoparticle	k [Wm^{-1}K^{-1})	ρ [kgm^{-3}]	c_p [Jkg^{-1}K^{-1}]	d_p [nm]	φ [–]
Cu	401	8933	385	50	2%
TiO_2	9	4250	686	50	2%
Cu-TiO_2	205	6591	482	50	1% – 1%

Results and discussion

The results for the performance of the solar dish collector are presented in figs. 2-7 with a brief way. These results correspond to a flow rate of 200 L/h, 25 °C ambient temperature and solar beam irradiation of 1000 W/m^2. In these figures, the value of the examined parameter for operation with pure thermal oil (Syltherm 800) is depicted in the left axis, while the variation of it for the nanofluid cases is given in the right axis. This presentation way is able to give clearly performance enhancement with the use of nanofluids.

Figure 2 depicts the Nusselt number variation for the pure oil case with the inlet temperature level. The Nusselt number is found to increase from 44 to 132. Moreover, the Nusselt number enhancement with the use of nanofluids is given in this figure. The heist Nusselt number enhancement is found for the hybrid nanofluid and it is up to 300%, while the mono nanofluids present similar enhancements close to 50%. At low temperatures, the Oil/TiO_2 has a higher Nusselt number, while in high temperatures (over 225 °C), the Oil/Cu present a rough surpass over the Oil/TiO_2.

The Nusselt number enhancement leads to heat transfer coefficient enhancement, as eq. (14) shows. Figure 3 indicates that the heat transfer coefficient enhancement has the same values as for the Nusselt number. Moreover, it is important to state that the heat transfer coefficient increases for high temperature levels. The heat transfer coefficient is about 400 W/m^{2}K for 25 °C inlet temperature, while it is about 1200 W/m^{2}K for inlet temperature at 300 °C inlet temperature.

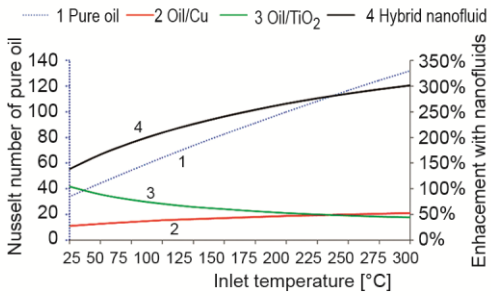

Figure 2. Nusselt number results for the examined cases and inlet temperature levels between 25 °C and 300 °C

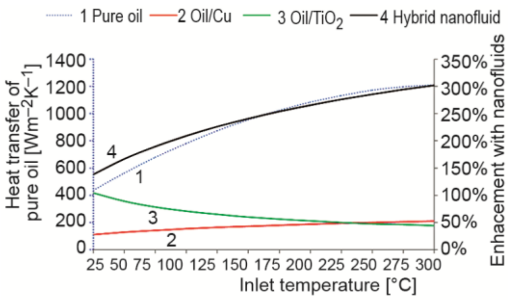

Figure 3. Heat transfer coefficient results for the examined cases and inlet temperature levels between 25 °C and 300 °C

This increase of the heat transfer coefficient is able to lead to lower receiver temperature, see eq. (5). This statement is validated with the results of fig. 4. These results indicate that there is a reduction in the receiver temperature up to 25% with the use of nanofluids. This reduction is getting lower at higher temperature levels because the absolute value of the receiver temperature increases due to the inlet temperature increase. In any case, the hybrid nanofluid leads to the highest decrease, with Oil/TiO_2 and Oil/Cu to follow, respectively.

The reduction of the receiver temperature has a direct impact on the thermal losses of the solar collector which present also an important reduction. Figure 5 proves that the thermal loss reduction can be up to 35% with hybrid nanofluid in low temperature levels. The thermal losses decrease is higher at lower inlet temperature because at these temperature levels the heat transfer coefficient is lower, see fig. 3, and so there is a lower enhancement margin with the use of nanofluids.

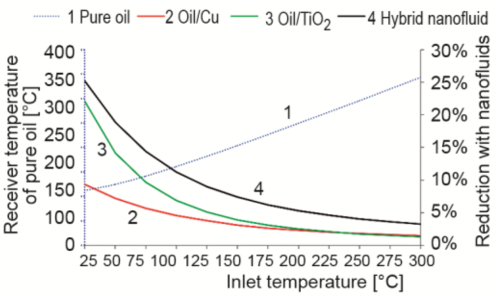

Figure 4. Receiver temperature results for the examined cases and inlet temperature levels between 25 °C and 300 °C

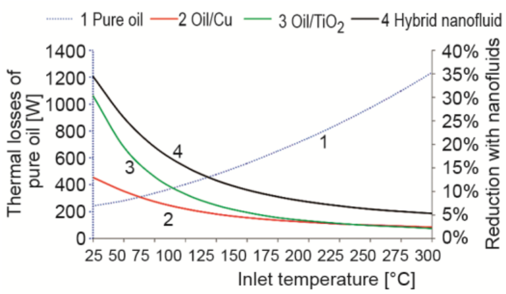

Figure 5. Thermal losses results for the examined cases and inlet temperature levels between 25 °C and 300 °C

The decrease in thermal losses leads to enhancement in the thermal efficiency, as fig. 6 depicts. The thermal efficiency with pure oil is ranged from 56.98% up to 66.64% and it decreases with the temperature increase. The thermal enhancements are generally from 0.4% up to 1.2%. The hybrid nanofluid presents the highest enhancement compared to the other nanofluids. The Oil/TiO_2 leads to higher thermal efficiency than the Oil/Cu for inlet temperature up to 225 °C. For inlet temperature over 225 °C, the Oil/TiO_2 leads to the lowest enhancements.

Similar results about the exergy efficiency enhancement are given in fig. 7. The exergy efficiency presents the maximum enhancement with the hybrid nanofluid, with Oil/TiO_2 to be the second choice up to 225 °C and after this temperature level, the Oil/Cu is the second choice. The exergy efficiency increase with the inlet temperature increase and it is ranged from 7.7% to 30.8%. Generally, the exergy efficiency is more enhanced than the thermal efficiency.

The tab. 2. includes the mean enhancements (or reductions) of the examined parameters for the three nanofluids compared to the pure oil case. These mean values have been calculated using the results of all the examined inlet temperature levels. The mean thermal efficiency enhancement for the hybrid nanofluid is found at 0.99%, while it is 0.42% with Oil/Cu and 0.56% with Oil/TiO_2. The mean exergy efficiency enhancement is 1.21% for hybrid nanofluid, 0.73% for Oil/TiO_2 and 0.53% for Oil/Cu.

Table 2. Mean variation of various parameters for the examined nanofluids

Parameter	Oil/Cu	Oil/TiO_2	Oil/(Cu-TiO_2)
Nu – enhancement	42.60%	63.52%	237.15%
h – enhancement	42.60%	63.52%	237.15%
T_r – decrease	3.82%	6.18%	9.44%
Q_{loss} – decrease	5.42%	8.61%	13.19%
η_{th} – enhancement	0.42%	0.56%	0.99%
η_{ex} – enhancement	0.53%	0.73%	1.21%

It is important to state that the enhancement of the Nusselt number takes high values (about 50% for the mono nanofluids and 237% for the hybrid nanofluid), while the thermal losses and receiver temperature reductions are lower (about 5%-10%). Moreover, the thermal and exergy efficiency enhancements are lower, close to 0.5%-1%. These results indicate that it is needed extremely high enhancements in the Nusselt number in order to increase the collector performance in solar dish collectors.

Lastly, it is crucial to state that the use of nanofluids is associated with various limitations which are associated with their high cost and the stability problems due to the agglomeration. Thus, there is a need for extra research in this domain in order to make nanofluids a commercial high efficient choice.

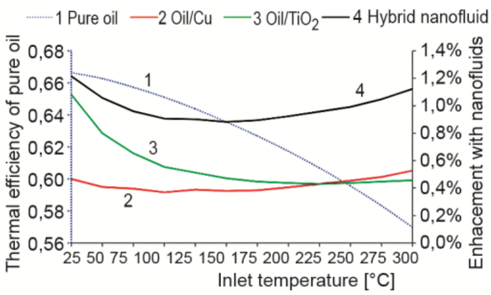

Figure 6. Thermal efficiency results for the examined cases and inlet temperature levels between 25 °C and 300 °C

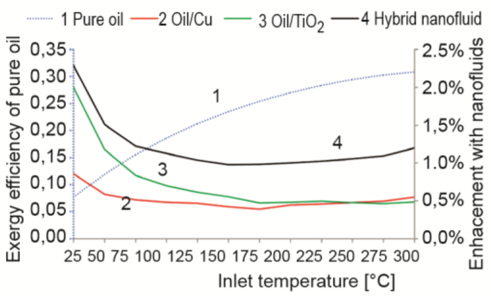

Figure 7. Exergy efficiency results for the examined cases and inlet temperature levels between 25 °C and 300 °C

Conclusions

The objective of this study is to investigate the impact of mono and hybrid nanofluids in a solar dish collector with the spiral absorber. The examined mono nanofluids are Oil/Cu and Oil/TiO_2 with 2% nanoparticle concentration in every case. The examined hybrid nanofluid is Oil/(Cu-TiO_2) with 1% Cu and 1% TiO_2. The solar collector is examined under turbulent flow conditions (flow rate of 200 L per hours) for inlet temperatures from 25 °C up to 300 °C. The most important conclusions from this work are listed.

- All the examined nanofluids lead to increase thermal and exergy performance of the solar dish collector, with the hybrid nanofluid to leads to the highest performance.
- The mean thermal efficiency enhancement with the hybrid nanofluid is 0.99% while it is 0.42% with Oil/Cu and 0.56% with Oil/TiO_2.
- The mean exergy efficiency enhancement with the hybrid nanofluid is 1.21% while it is 0.53% with Oil/Cu and 0.73% with Oil/TiO_2. The exergy efficiency enhancements are higher than the respective thermal efficiency enhancements.
- The performance enhancement is explained by the Nusselt number enhancement which leads to lower receiver temperature and consequently to lower thermal losses of the collector. The mean enhancement of the Nusselt number is found 237.15% for the hybrid nanofluid, while it is found 42.60% with Oil/Cu and 63.52% with Oil/TiO_2.

The last conclusion of this work is that the use of nanofluids is able to enhance both thermal and exergy performance, especially at high temperatures. The use of hybrid nanofluid seems to be the best solution and so more work has to be conducted in this direction. In any case, important problems which are associated with the nanofluids operations (like their high cost and the agglomeration problems) have to be faced before their commercial use.

Acknowledgment

This paper is done within the research framework of the research project: III42006 – Research and development of energy and environmentally highly effective polygeneration systems based on renewable energy resources. The project is financed by the Ministry of Education, Science and Technological Development of the Republic of Serbia. The experiments were conducted at the Faculty of Mechanical Engineering in Nis, Laboratory for Thermal and Process Engineering. Moreover, E. Bellos would like to thank *Bodossaki Foundation* for its financial support and D. Vasiljevic would like to acknowledge support from the Ministry of Education, Science and Technological Development of the Republic of Serbia under Project No. III45016.

Nomenclature

A – area, [m^2]
c_p – specific heat capacity under constant pressure, [$Jkg^{-1}K^{-1}$]
D – diameter, [m]
d_p – nanoparticle diameter, [m]
G_b – solar beam irradiation, [Wm^{-2}]
h – convection heat transfer coefficient, [$Wm^{-2}K^{-1}$]
h_{out} – convection heat transfer coefficient between the absorber and ambient air, [W/m^2K]
k – thermal conductivity, [$W/m^{-1}K^{-1}$]
k_b – Boltzmann's constant ($\sim 1.3806 \cdot 10^{-23}$), [$JK^{-1}$]
m – mass-flow rate, [kgs^{-1}]
Nu – mean Nusselt number, [–]
Pr – Prandtl number, [–]
Q – heat transfer rate, [W]
Re – Reynolds number of the fluid, [–]
Re_d – Reynolds number of the nanoparticle, [–]
T – temperature, [°C]

Greek symbols

ε – emittance, [–]
η – efficiency, [–]
μ – dynamic viscosity, [Pa·s]
ρ – density, [kgm^{-3}]

σ – Stefan-Boltzmann constant (= $5.67 \cdot 10^{-8}$) [Wm^{-2} K^{-4}]
φ – total volumetric nanoparticle concentration, [–]
φ_1 – volumetric Cu concentration in the hybrid nanofluid, [–]
φ_2 – volumetric TiO_2 concentration in the hybrid nanofluid, [–]

Subscripts and superscripts

a – aperture
am – ambient
bf – base fluid
ex – exergetic
fm – mean fluid
in – inlet
loss – losses
nf – nanofluid
np – nanoparticle
o – reference
opt – optical
out – outlet
r – receiver
s – solar
Sun – Sun
th – thermal
u – useful

Acronym

EES – Engineering Equator Solver

References

[1] Fuqiang, W. *et al.*, Progress in Concentrated Solar Power Technology with Parabolic trough Collector System: A Comprehensive Review, *Renewable and Sustainable Energy Reviews, 79* (2017), Nov., pp. 1314-1328
[2] Selimli, S. *et al.*, Solar Vacuum Tube Integrated Seawater Distillation – an Experimental Study, *Facta Universitatis – Series Mechanical Engineering, 14* (2016), 1, pp. 113-120
[3] Daabo, A. M. *et al.*, The Optical Efficiency of Three Different Geometries of a Small Scale Cavity Receiver for Concentrated Solar Applications, *Applied Energy , 179* (2016), Oct., pp. 1081-1096
[4] Senthil, R., Cheralathan, M., Effect of the Phase Change Material in a Solar Receiver on Thermal Performance of Parabolic Dish Collector, *Thermal Science, 21* (2017), 6, pp. 2803-2812
[5] Bellos, E. *et al.*, The Impact of Internal Longitudinal Fins in Parabolic trough Collectors Operating with Gases, *Energy Conversion and Management, 135* (2017), Mar., pp. 35-54
[6] Li, S., *et al.*, Optical Performance of a Solar Dish Concentrator/Receiver System: Influence of Geometrical and Surface Properties of Cavity Receiver, *Energy, 113* (2016), Oct., pp., 95-107
[7] Bellos, E. *et al.*, Energetic, Exergetic and Financial Evaluation of a Solar Driven Absorption Chiller – A Dynamic Approach, *Energy Conversion and Management, 137* (2017), Apr., pp. 34-48
[8] Loni, R., *et al.*, Performance Study of a Solar-Assisted Organic Rankine Cycle Using a Dish-Mounted Rectangular-Cavity Tubular Solar Receiver, *Applied Thermal Engineering, 108* (2016), Sept., pp. 1298-1309
[9] Reddy, K.S. *et al.*, Combined Heat Loss Analysis of Solar Parabolic Dish – Modified Cavity Receiver for Superheated Steam Generation, *Solar Energy, 121* (2015), Nov., pp. 78-93
[10] Przenzak, E. *et al.*, The Numerical Model of the High Temperature Receiver for Concentrated Solar Radiation, *Energy Conversion and Management, 125* (2016), Oct., pp. 97-106.
[11] Zhu, J. *et al.*, Experimental Study of the Energy and Exergy Performance for a Pressurized Volumetric Solar Receiver, *Applied Thermal Engineering, 104* (2016), July, pp. 212-221
[12] Daabo, A. M. *et al.*, The Effect of Receiver Geometry on the Optical Performance of a Small-Scale Solar Cavity Receiver for Parabolic Dish Applications, *Energy, 114* (2016), Nov., pp. 513-525
[13] Yu, T. *et al*., Thermochemical Storage Performances of Methane Reforming with Carbon Dioxide in Tubular and Semi-Cavity Reactors Heated by a Solar Dish System, *Applied Energy, 185* (2017), 2, pp. 1994-2004
[14] Loni, R. *et al.*, Thermodynamic Analysis of a Solar Dish Receiver Using Different Nanofluids, *Energy, 133* (2017), Aug., pp. 749-760
[15] Loni, R. *et al.*, Thermal and Exergy Performance of a Nanofluid-Based Solar Dish Collector with Spiral Cavity Receiver, *Applied Thermal Engineering, 135* (2018), May, pp. 206-217
[16] Pavlovic, S. *et al.*, Exergetic Investigation of a Solar Dish Collector with Smooth and Corrugated Spiral Absorber Operating with Various Nanofluids, *Journal of Cleaner Production, 174* (2018), Feb., pp. 1147-1160
[17] Pakhare, J. N. *et al.*, Experimental Performance Evaluation of a Parabolic Solar Dish Collector with Nanofluid, in: *Concentrated Solar Thermal Energy Technologies*, Springer, New York, USA, 2018, pp. 115-123

[18] Rajendran, D. R. *et al.*, Experimental Studies on the Effect of Enhanced Thermal Conductivity of SiC+Water Nanofluid in the Performance of Small Scale Solar Parabolic Dish Receiver, *Int. J. Nanosci., 17* (2018), ID 1760025
[19] Sarkar, J. *et al.*, A Review on Hybrid Nanofluids: Recent Research, Development and Applications, *Renewable and Sustainable Energy Reviews, 43* (2015), Mar., pp. 164-177
[20] Bellos, E., Tzivanidis, C., Thermal Analysis of Parabolic trough Collector Operating with Mono and Hybrid Nanofluids, *Sustainable Energy Technologies and Assessments, 26* (2018), Apr., pp. 105-111
[21] Minea, A. A., El-Maghlany, W. M., Influence of Hybrid Nanofluids on the Performance of Parabolic trough Collectors in Solar Thermal Systems: Recent Findings and Numerical Comparison, *Renewable Energy, 120* (2018), May, pp. 350-364
[22] Stefanovic, V. P. *et al.*, A Detailed Parametric Analysis of a Solar Dish Collector, *Sustainable Energy Technologies and Assessments, 25* (2018), Feb., pp. 99-110
[23] Pavlovic, S. *et al.*, Experimental Investigation and Parametric Analysis of a Solar Thermal Dish Collector with Spiral Absorber, *Applied Thermal Engineering, 121* (2017), July, pp. 126-135
[24] Pavlovic, S. *et al.*, Experimental and Numerical Investigation on the Optical and Thermal Performance of Solar Parabolic Dish and Corrugated Spiral Cavity Receiver, *Journal of Cleaner Production, 150* (2017), May, pp. 150:75-92
[25] Pavlovic, S. R. *et al.*, Optical Analysis and Performance Evaluation of a Solar Parabolic Dish Concentrator, *Thermal Science, 20* (2016), Suppl. 5, pp. S1237-S1249
[26] Pavlovic, S. R. *et al.*, Design, Simulation and Optimization of a Solar Dish Collector Spiral-Coil Thermal Absorber, *Thermal Science, 20* (2016), 4, pp. 1387-1397
[27] ***, F-Chart Software, Engineering Equation Solver (EES); 2015. (http://www.fchart.com/ees)
[28] ***, https://www.loikitsdistribution.com/files/syltherm-800-technical-data-sheet.pdf
[29] ***, http://www.almecogroup.com/en
[30] Petela, R., Exergy of Undiluted Thermal Radiation, *Solar Energy, 74* (2003), 6, pp. 469-488
[31] Bellos, E., Tzivanidis, C., Parametric Analysis and Optimization of an Organic Rankine Cycle with Nanofluid Based Solar Parabolic trough Collectors, *Renewable Energy, 114(B)* (2017), Dec., pp. 1376-1393
[32] Bellos, E., Tzivanidis, C., Parametric Investigation of Nanofluids Utilization in Parabolic trough Collectors, *Thermal Science and Engineering Progress, 2* (2017), June, pp. 71-79
[33] Khanafer, K., Vafai, K., A Critical Synthesis of Thermophysical Characteristics of Nanofluids, *International Journal of Heat and Mass Transfer, 54* (2011), 19, pp. 4410-4428
[34] Maxwell, J. C. A., *Treatise on Electricity and Magnetism*, 2nd, Clarendon Press, Oxford, UK, 1881
[35] Batchelor, G., The Effect of Brownian Motion on the Bulk Stress in a Suspension of Spherical Particles, *J. Fluid Mech., 83* (1977), 1, pp. 97-117
[36] Leinhard IV, J., Leinhard V, J., *A Heat Tranfer Textbook*, 4th, Philogiston Press, Cambridge, Mass., USA, 2012
[37] Li, Q., Xuan, Y., Convective Heat Transfer and Flow Characteristics of Cu-Water Nanofluid, *Science in China (Series E), 45* (2002), 4, pp. 409-416
[38] Duangthongsuk, W., Wongwises, S., An Experimental Study on the Heat Transfer Performance and Pressure Drop of TiO_2-Water Nanofluids Flowing under a Turbulent Flow Regime, *International Journal of Heat and Mass Transfer, 53* (2010), 1-3, pp. 334-344
[39] Madhesh, D., *et al.*, Experimental Investigation on Convective Heat Transfer and Rheological Characteristics of Cu–TiO_2 Hybrid Nanofluids, *Experimental Thermal and Fluid Science, 52* (2014), Jan., pp. 104-115
[40] Bellos, E. *et al.*, The Use of Nanofluids in Solar Concentrating Technologies: A Comprehensive Review, *Journal of Cleaner Production, 196* (2018), Sept., pp. 84-99

Paper submitted: March 25, 2018
Paper revised: August 31, 2018
Paper accepted: September 2, 2018